Journal of Alloys and Compounds 873 (2021) 159758

Contents lists available at ScienceDirect

Journal of Alloys and Compounds

journal homepage: www.elsevier.com/locate/jalcom

Sc modification induced short-range cation ordering and high microwave dielectric performance in $ZnGa_2O_4$ spinel ceramics

Xiaochi Lu[a,b], Bin Quan[c], Kailai Zheng[a,e], Peng Chu[a], Jian Wang[a], Guangxu Shen[a], Qitu Zhang[d], Feng Xu[a,*]

[a] College of Electronic and Optical Engineering & College of Microelectronics, Nanjing University of Posts and Telecommunications, Nanjing 210023, PR China
[b] National and Local Joint Engineering Laboratory of RF Integration and Micro-Assembly Technology, PR China
[c] Institute of Advanced Materials and Flexible Electronics (IAMFE), School of Chemistry and Materials Science, Nanjing University of Information Science & Technology, Nanjing 210044, PR China
[d] College of Materials Science and Engineering, Nanjing Tech University, Nanjing 210009, PR China
[e] State Key Lab. of Millimeter Waves, Southeast University, Nanjing 210096, PR China

ARTICLE INFO

Article history:
Received 7 November 2020
Received in revised form 21 March 2021
Accepted 28 March 2021
Available online 8 April 2021

Keywords:
$ZnGa_2O_4$
Spinel
Sc^{3+} modification
Bond vibration
Microwave dielectric properties

ABSTRACT

Sc^{3+} (0,0.1,0.3,0.5,0.7 mol%) modified $ZnGa_2O_4$ (abbreviated Sc-ZGO) ceramics were synthesized by solid-state method. The relationship between microwave dielectric performance and bonds vibration has been systematically investigated. With Sc^{3+} modification, the ε_r of Sc-ZGO keeps steady (~10). While τ_f values (increasing from −71 ppm/°C to −39 ppm/°C) show linear correlation with Sc^{3+} concentration. And $Q\times f$ values climb up to a maximum value and then ramp down. The $Q\times f$ value of Sc-ZGO increased by almost 45% compared with normal spinel $ZnGa_2O_4$ ceramics. The enhancement of τ_f and $Q\times f$ on Sc modified $ZnGa_2O_4$ can be attributed to higher densification, however, further analysis elucidated that short-range cation ordering degree is another governing factor. The influence of Sc^{3+} modification on $ZnGa_2O_4$ bonds vibration has been discussed in detail. 5Sc-ZGO sintered at 1350 °C for 2 h exhibits the best microwave dielectric properties: ε_r = 9.9, $Q\times f$ = 124,147 GHz, tanδ = 7.98 × 10^{-5}, and τ_f = −56 ppm/°C (@9.9 GHz).
© 2021 Elsevier B.V. All rights reserved.

1. Introduction

Spinel-type compounds AB_2O_4 have been extremely investigated in science and technical fields such as phosphor [1,2], catalysts [3,4], semiconductors [5,6], superconductors [7,8] and microwave dielectric materials [9–12]. Among these applications, microwave dielectric materials in high frequency (5G) is one of the most important applications with wide investigations. The framework of Spinel-type compounds has close packed tetrahedral (AO_4 or BO_4) and octahedral (BO_6 or AO_6). This type of crystal structure has different variabilities in cation ordering such as common spinel (AB_2O_4), inverse spinel ($B(AB)O_4$) and mixed-type spinel. So far, spinel structured ceramics for high frequency application include M_2SnO_4 [13,14], M_2SiO_4 [15,16], MAl_2O_4 (M=Zn, Mg) [17,18] and MGa_2O_4 (M = Zn, Mg) [19–23].

However, the development and application of M_2SnO_4 are limited by large negative τ_f and low $Q\times f$. As for M_2SiO_4, the critical synthesis condition limited its application. Although the $Q\times f$ of MAl_2O_4 can exceed to 60,000 GHz, its sintering temperature is relatively high. Cause most of the spinel ceramics need high sintering temperature for about 1600 °C. Considering environment friendly materials, explorations in lower sintering temperature by materials design and composition engineering are increased. Compared with M_2SnO_4, M_2SiO_4 and MAl_2O_4 (M=Zn, Mg), MGa_2O_4 have good microwave dielectric properties, lower sintering temperature and a wide sintering temperature region. Therefore, MGa_2O_4 (M=Zn,Mg) materials are promising candidates for high frequency (5G) applications.

For MGa_2O_4 (M=Zn, Mg) materials, $ZnGa_2O_4$ is normal spinel and $MgGa_2O_4$ is mixed-type spinel. Thus, the crystal structure of $MgGa_2O_4$ is more complexed than the former one and the mixed proportion varied with synthesis conditions which brings more difficulties to reveal relationships among synthesis conditions, modification, crystal structure and microwave dielectric properties. Hence, $ZnGa_2O_4$ with normal spinel structure got our attention. It is reported that $ZnGa_2O_4$ possesses lower sintering temperature (1400 °C), large sintering range (1300 °C −1500°C) with excellent dielectric performance (ε_r = 9.8, $Q\times f$ = 83,000 GHz, τ_f = −71 ppm/°C)

* Corresponding author.
E-mail address: feng.xu@njupt.edu.cn (F. Xu).

https://doi.org/10.1016/j.jallcom.2021.159758
0925-8388/© 2021 Elsevier B.V. All rights reserved.

[10]. However, relatively large negative τ_f (−71 ppm/°C), and the relatively large tanδ (19×10^{-5}) are two difficulties in the application of $ZnGa_2O_4$ microwave dielectric ceramics.

For microwave dielectric materials with high density and good crystallinity, the initial temperature coefficient at resonant frequency (τ_f) can be got through formula (1) as follows [24]:

$$\tau_f = -\left(\frac{1}{2}\tau_\varepsilon + \frac{1}{2}\tau_\mu + \alpha_L\right) \quad (1)$$

Thus, the permittivity coefficient (τ_ε), permeability coefficient (τ_μ), coefficient of thermal expansion (α_L) are three considerable factors to determine τ_f. In our previous study, TiO_2 was applied to form TiO_2-$ZnGa_2O_4$ composite ceramics to adjust τ_ε, and through this method near zero τ_f was obtained [19]. Another study applied Mn to modified the τ_μ of $ZnGa_2O_4$ and it successfully shifted τ_f from −71 ppm/°C to −12 ppm/ °C [20].

To achieve a high signal noise ratio, resonators should possess higher $Q\times f$. $1/Q$ is the total loss (tanδ) and can be figured out through formula 2 [25]. $1/Q_d$, $1/Q_c$, $1/Q_r$, and $1/Q_{ext}$ are related to dielectric, conductor, radiation and external power loss, respectively.

$$\frac{1}{Q} = \frac{1}{Q_d} + \frac{1}{Q_c} + \frac{1}{Q_r} + \frac{1}{Q_{ext}} \quad (2)$$

Classically, materials with close packed, ordered structure, high density, good crystallinity and fine morphology possess low tanδ because of lower vibration tanδ, grain boundary tanδ and impurity loss. In our previous study, Cr^{3+} doped $ZnGa_2O_4$ obtain excellent microwave dielectric properties due to the higher density and higher short-range cation ordering [21]. Cu^{2+} was also applied to form Cu-ZGO solid solutions and obtain mixed spinel structure, the higher density and higher short-range cation ordering contribute to the higher $Q\times f$ [22,23].

Rare earth (RE) elements possess special atomic structure, physical and chemical properties which is mainly caused by their 4 f electron configuration. The special structure of RE elements leads to special optical, electrical, magnetic and thermal properties. And the application of RE elements in ceramic materials has made great progress. Thus, RE modification have been applied extensively to control microstructures, crystal structures and dielectric properties, especially in piezoelectric ceramics and microwave dielectric ceramics like PZT [26], Ca/BaO-Ln_2O_3-TiO_2 [27] and CaO-Ln_2O_3-TiO_2-Li_2O [28]. The most used RE elements are Nd, Y, Sm and Ce, however, Sc has not yet been studied in this respect.

Based on the above discussion, Sc modified $ZnGa_2O_4$ (abbreviated Sc-ZGO) were designed to achieve higher $Q\times f$ and near zero τ_f. As a result, we obtain a low $\varepsilon_r \sim 10$ at 13 GHz, with sintering temperature at 1350 °C which is lower than most of spinel ceramics without sintering additives. The microwave dielectric performance of Sc-ZGO, demonstrating low tanδ, and a near zero τ_f was achieved. Thus, it can provide guidance on the enhancement of spinel-type microwave dielectric ceramics properties.

2. Materials and methods

2.1. Sample preparation

Solid state reactions were adopted to prepare Sc-ZGO with Sc content range from 0.1 mol to 0.7 mol%. According to the Sc-ZGO chemical formula, analytical grade Sc_2O_3, Ga_2O_3, and ZnO were weighted and ball milled in polyethylene jars for one day with ethanol. Then the mixtures were dried at 80 °C for one day and calcined at 1000 °C for 2 h. The green pellets with diameter~13 mm and thickness ~6 mm, was obtained under an uniaxial pressure ~75 MPa for 1 min, and then sintered at 1300–1450 °C for 2 h in high-temperature electric furnace (KSX4–16, Allfine, Wuxi, China) to obtain ceramic pellets.

2.2. Characterization

The micromorphology of Sc-ZGO was detected by a scanning electron microscope (SEM) (Hitachi SU8010, Japan). Archimedes' method was applied to measure the density of the given samples. Phase composition and evolution of Sc-ZGO ceramics were identified via X-ray diffraction (XRD) (Rigaku Cu, RigakuD/Max 2500, Japan), XRD refinement was applied using the General Structure Analysis System (PC-GSAS) software, and Raman spectroscopy (Raman) (HR800, Horiba Labram, 514 nm He-Cd laser, 20 mW laser power). The high-resolution TEM (HRTEM) images and selected-area electron diffraction (SAED) patterns were achieved at 200 kV using a transmission electron microscope (JEM-2100, JEOL). X-ray photoelectron spectrometer (XPS) (ESCALAB 250, Thermo Fisher, UK) was employed to collect XPS data to reveal elements chemical status with Al-Kα as its X-ray source. The microwave dielectric performance: ε_r, tanδ, f and τ_f, were measured using the cavity resonator method [29] via a Lightwave Component Analyzer (Hewlett Packard 8703 A, 1550 nm/130 MHz to 20 GHz). A NICOLET 5700 FT-IR spectrometer (Thermo, America) were applied to get the Fourier transform infrared (FT-IR) spectrum.

3. Results and discussion

3.1. Microstructure of Sc-ZGO ceramics

The microstructures and relative density of Sc-ZGO ceramics sintered at 1350 °C for 2 h are shown in Fig. 1(a-e), and (f) shown the EDS spectrum of 5Sc-ZGO. As the Sc modification content increasing, the average size varied slightly, however, the relative density is different. It first increased with increasing Sc^{3+} content from 0.1 to 0.7 mol% and achieved the highest density at 5Sc-ZGO, then decreased at 7Sc-ZGO. Thus, Sc^{3+} modification also improves the densification of $ZnGa_2O_4$. A relative density of 97% is reachable with Sc^{3+} content ranging from 0 to 0.7 mol%.

3.2. Crystal structure and cation distribution

The XRD patterns of Sc-ZGO ceramics with Sc^{3+} modification content ranging from 0 to 0.7 mol% are shown in Fig. 2(a). Fig. 2(b) is the enlarged XRD patterns at $2\theta = 35.2–36.0$. All the samples can be indexed as pure spinel structured $ZnGa_2O_4$ (JCPDS card no. 86–0413). Due to the Sc modification, the main diffraction peak (~35.6°) shifts to higher diffraction degree which reveals lattice contraction in the Sc-ZGO crystals.

Fig. 2(c) shows an exemplar HRTEM image together with the SAED pattern in the inset, taken from 5Sc-ZGO. The lattice spacing is 0.48 nm which corresponds to the spacing between the (111) planes of spinel structured $ZnGa_2O_4$. SAED pattern can provide further insight into the ceramic crystal structure. It can be indexed as a spinel structure with Face-Centered Cubic symmetry and a zone axis of $[1\bar{1}0]$. The sharp diffraction spots in the SAED pattern, indicating Sc-ZGO possesses good crystallinity.

Confirming by previous XRD analysis, the higher Sc^{3+} concentration means the larger lattice contraction. Fig. 2(d) shows XRD refinement of 7Sc-ZGO. It confirms that 7Sc-ZGO possesses pure spinel structure. Thus, all of these evidences indicate that Sc-ZGO (Sc^{3+} content from 0 to 0.7 mol%) is a solid solution.

XPS spectrum of 5Sc-ZGO sintered at 1350 °C for 2 h are shown in Fig. 3. These 5 peaks, Ga 3d, Sc 2p, O 1 s, Zn 2p and Ga 2p peaks can be clearly seen in the full XPS spectrum in Fig. 3(a). And the reflection peaks at 19.8 eV, 530.5 eV, and 1044 eV binding energy in Fig. 3(c-d), are corresponding to Ga 3d, O 1 s, and Zn 2p, respectively. These means Sc existed as trivalent state in Sc-ZGO, and Sc^{3+} modification didn't affect bond valence of $ZnGa_2O_4$.

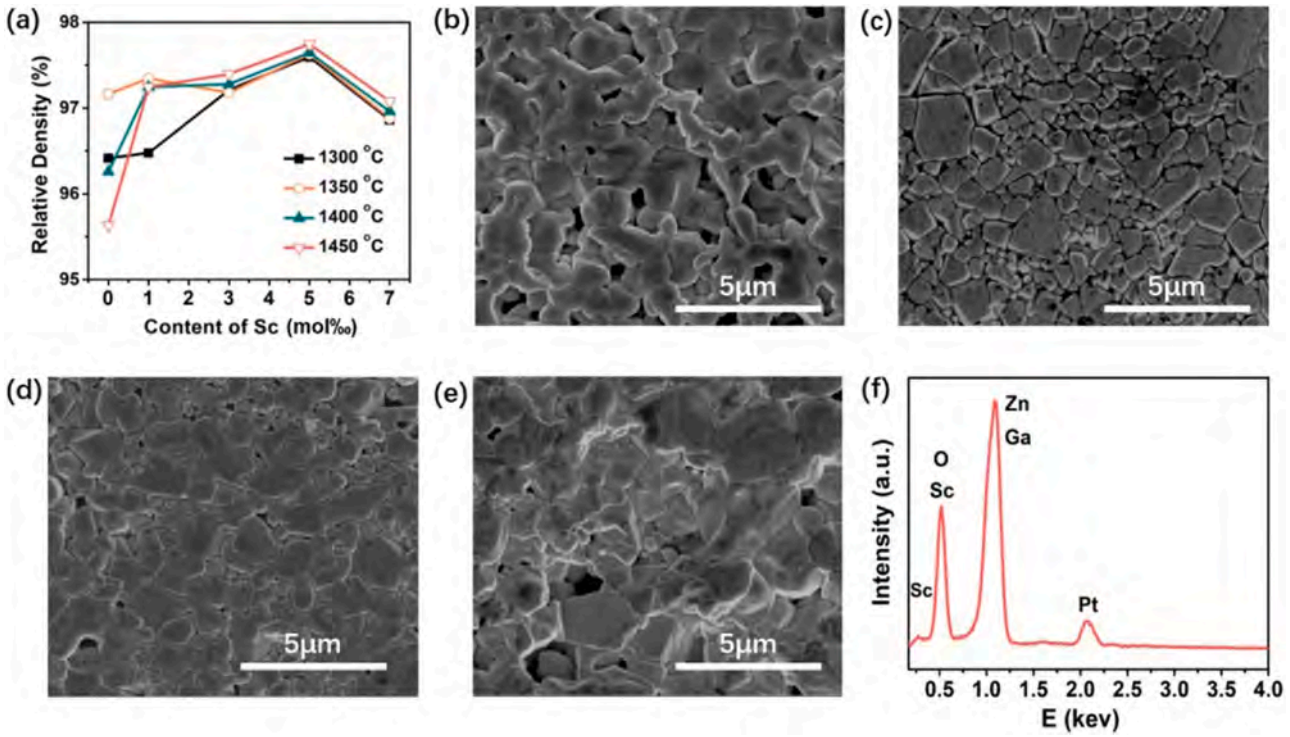

Fig. 1. (a) Relative density of Sc-ZGO, SEM images of Sc-ZGO sintered at 1350 °C for 2 h and (b–e) are 1Cr-ZGO, 3Cr-ZGO, 5Cr-ZGO, and 7Cr-ZGO, respectively. (f) EDS of 5Sc-ZGO.

3.3. Microwave dielectric properties

The microwave dielectric properties of Sc-ZGO sintered at 1350 °C for 2 h, have been investigated and the results are shown in Fig. 4. As is shown in Fig. 4(a), the *Q*×*f* values of Sc-ZGO are strongly depend on Sc^{3+}modification. It reaches the maximum value of 124,147 GHz at 5Sc-ZGO, and then decreased with Sc^{3+} modification. According to our previous study, the *Q*×*f* value of Sc-ZGO increased by almost 1.45 times compared with unmodified $ZnGa_2O_4$. Therefore, Sc^{3+} modification is an effective way to improve *Q*×*f* values of

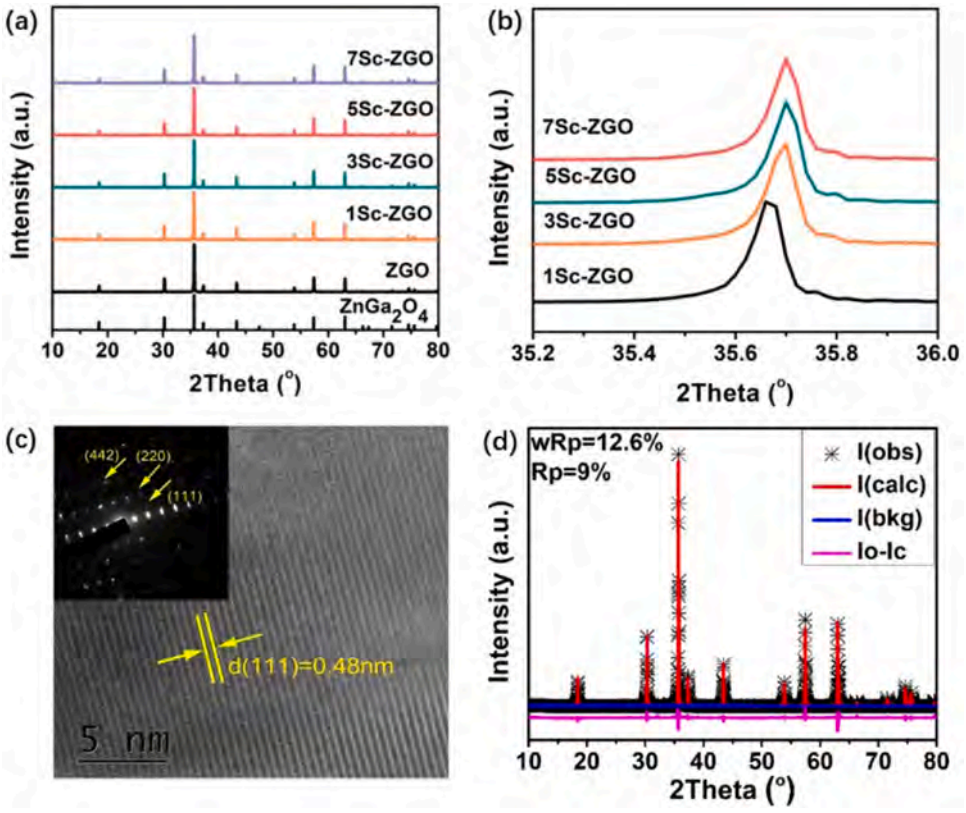

Fig. 2. (a) XRD pattern of Sc-ZGO sintered at 1350 °C for 2 h, (b) enlarged XRD patterns at 2θ= 35.2–36.0, and (c) TEM image of 5Sc-ZGO. (d) XRD Refinement of 7Sc-ZGO.

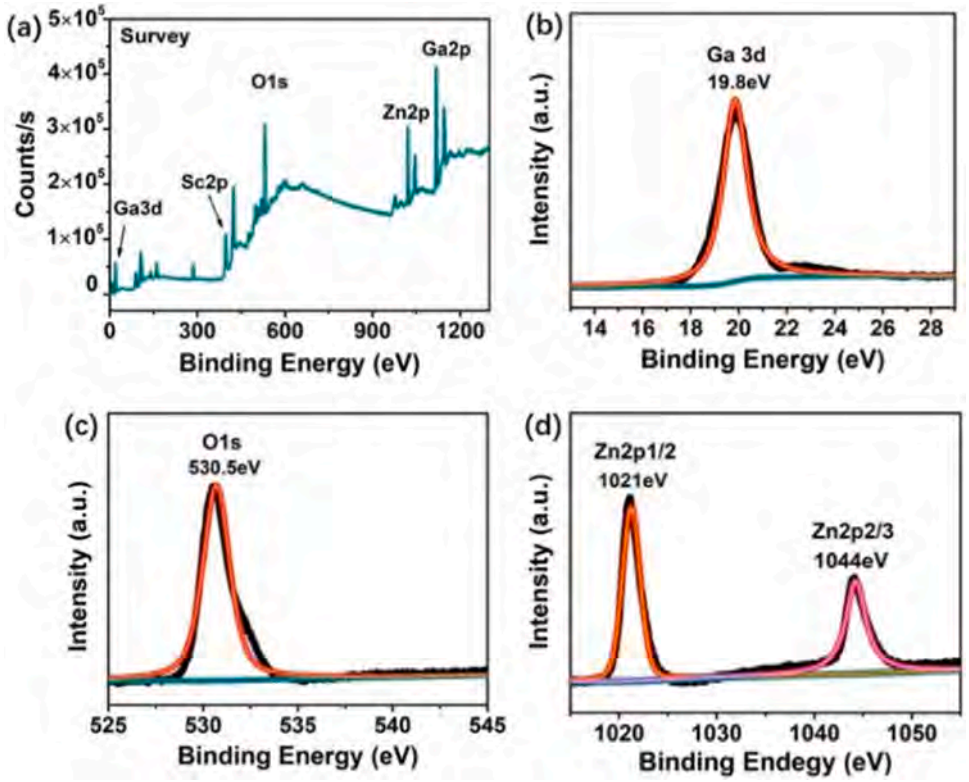

Fig. 3. XPS spectra of the middle part of $ZnGa_2O_4$ sintered at 1350 °C for 2 h, (a) full spectra, (b) Ga, (c) O, (d) Zn.

$ZnGa_2O_4$. As already shown in Fig. 1(a), the relative density of Sc-ZGO is increased with Sc^{3+} modification. It is reasonable to note that the $Q{\times}f$ values are higher for those ceramics with Sc^{3+} content range from 0.1 to 0.5 mol%, since higher density always benefits $Q{\times}f$. Fig. 4(b) displays τ_f value of Sc-ZGO sintered at 1350 °C for 2 h. The τ_f is −71 ppm/°C for pure ZGO, and then it increases linearly to −39 ppm/°C with Sc^{3+} modification. Due to the decrease of $Q{\times}f$, further addition didn't apply to achieve near zero τ_f. Therefore, doping

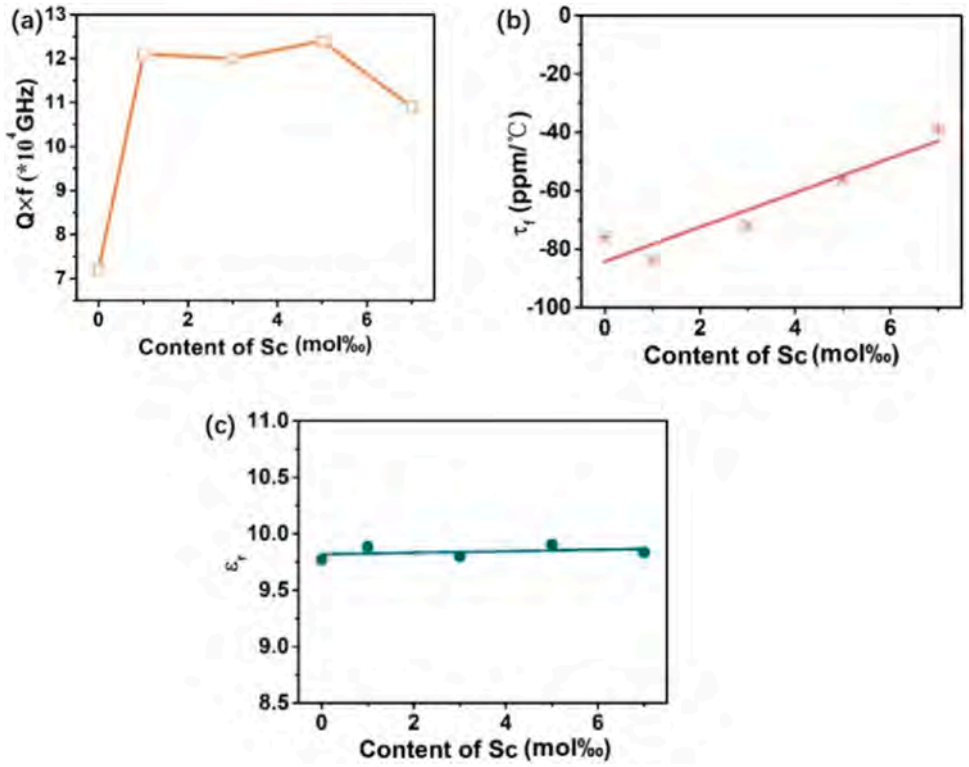

Fig. 4. Effect of Sc^{3+} modification on the microwave dielectric properties of $ZnGa_2O_4$ sintered at 1350 °C for 2 h. (a) quality factor ($Q{\times}f$) at various sintering temperatures, (b) temperature coefficient at resonant frequency (τ_f), and (c) dielectric constant (ε_r).

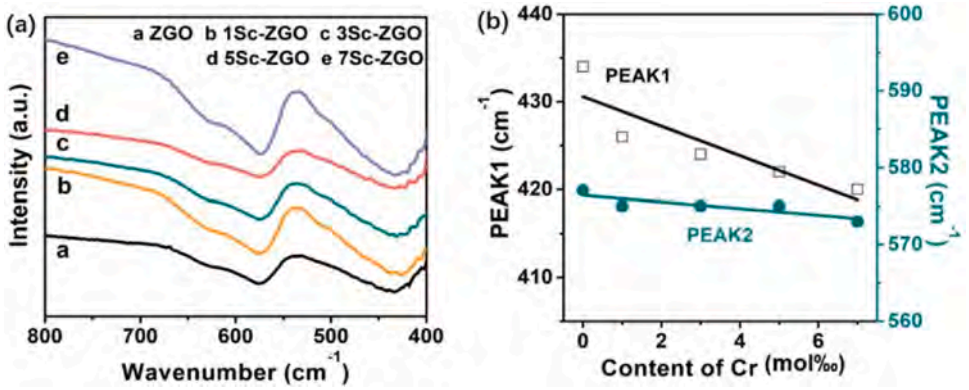

Fig. 5. (a) FT-IR spectra of Sc-ZGO, (b) the FT-IR peak positions and dielectric constant (ε_r) of the Cr-ZGO ceramics as a function of Sc content, sintered at 1350 °C for 2 h.

tiny Sc^{3+} (ppt) to improve both $Q{\times}f$ and τ_f, then applied magnetic ion such as Mn^{2+} or compounds like TiO_2 to further shift τ_f can both achieve great microwave dielectric performance and keep cost down. ε_r follows Clausius–Mossotti equation which determined by polarizabilities and molecular volume as formula (3). Due to Sc doping content is tiny (from 0.1 mol% to 0.7 mol%), and the α_m of Sc^{3+} is similar with Ga^{3+}. Thus, the ε_r of Sc-ZGO keeps steady with Sc modification.

$$\varepsilon_r = [3/(1\text{-}b\alpha_m/V_m)]\text{-}2 \quad (3)$$

3.4. FT-IR and Raman analysis on the spinel structure

FT-IR spectra of Sc-ZGO sintered at 1350 °C for 2 h is exhibited in Fig. 5(a). Two absorption bands: 420 cm^{-1} (labeled as PEAK1) and 570 cm^{-1} (labeled as PEAK2) were observed. Both PEAK1 and PEAK2 are belongs to T_{1u} IR-active mode. These two T_{1u} modes are induced predominantly by the vibrations of the octahedral site [30]. Hence, FT-IR spectrum can reflect the octahedral distortion in Sc-ZGO crystal structure. The absorption bands shift to lower wave number with Sc^{3+} content increasing which can be observed in Fig. 5(b), both for PEAK1 (from 434 cm^{-1} to 420 cm^{-1}) and PEAK2 (from 577 cm^{-1} to 573 cm^{-1}). These two FT-IR peaks shift was sensitive to Sc^{3+} and shown linear correlation with Sc^{3+} concentration, which means FT-IR shift were caused by Sc modification. Cause FT-IR absorption demonstrate bond vibration, the linear correlation between Sc^{3+} modification and FT-IR shift reflects that Sc^{3+} modification effectively influence ZGO bond vibration.

Fig. 6(a) exhibits the Raman spectrum of Sc-ZGO. Two peaks: T_{2g} phonon mode at ~607 cm^{-1} and A_{1g} phonon mode at ~712 cm^{-1} can be clearly seen which is consistent with $ZnGa_2O_4$ Raman characterization reported by Wiglusz [31]. The two T_{2g} and A_{1g} phonon modes in Fig. 6(a) are the first order Raman modes. T_{2g} phonon mode is the breathing mode of the octahedral site, and A_{1g} phonon mode is the stretching vibration in the tetrahedral site, respectively.

For perovskite materials, the full width at half maxima (FWHM) of Raman phonon mode is indicative of the short-range cation ordering and can be used to explain tanδ variety [22–35]. Perovskite materials with higher short-range cation ordering degree usually possess lower Raman FWHM and higher $Q{\times}f$. As perovskite and spinel materials have a similar crystal structure, it can be supposed that the tanδ of spinel structured materials has a correlation with Raman FWHM. The FWHM of the A_{1g}, T_{2g} phonon modes and tanδ of Sc-ZGO have been compiled in Fig. 6(b–c). The Raman shifts of the A_{1g} and T_{2g} phonon

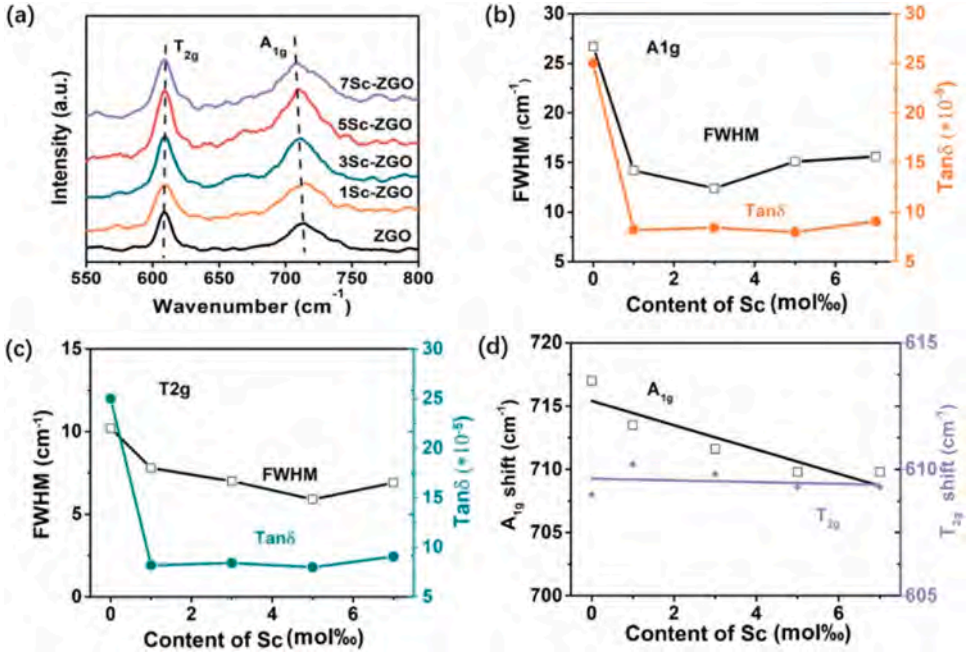

Fig. 6. (a)Raman spectra of Cr^{3+} modified $ZnGa_2O_4$, (b) FWHM value of the A_{1g} mode and dielectric loss (tanδ), (c) FWHM value of the T_{2g} mode and dielectric loss (tanδ), (d) A_{1g} shift and T_{2g} shift of Sc-ZGO ceramics as a function of Sc^{3+} concentration, sintered at 1350 °C for 2 h.

modes, and ε_r with increasing Sc^{3+} modification is compiled in Fig. 6(d). As FT-IR shift discussed above, these two Raman modes shift was sensitive to Sc^{3+} and shown linear relation with Sc^{3+} content, which means Raman modes shift was caused by Sc^{3+} modification. Cause Raman modes also demonstrate bond vibration, and have complementary relationship with FT-IR modes. The linear correlation between Sc^{3+} modification and Raman modes shift reflects that Sc^{3+} modification effectively influence ZGO bond vibration.

4. Conclusions

Sc-ZGO with excellent microwave dielectric properties have been successfully synthesized via solid state method. Due to the tiny modification concentration and ionic polarization, with Sc^{3+} modification, the ε_r of Sc-ZGO ceramics keeps steady. The $Q\times f$ value of Sc-ZGO ceramics ramp up to a maximum at 0.5 mol% Sc^{3+} modification and then ramp down continuously. In the Sc^{3+} content range from 0 to 0.7 mol%, $Q\times f$ increased from 83,000 GHz to 124,147 GHz and then decreased to 109,366 GHz. The τ_f value of Sc-ZGO increased linearly with Sc^{3+} concentration from −71 ppm/°C to −39 ppm/°C. Great microwave dielectric performance was achieved in 5Sc-ZGO spinel ceramics sintered at 1350 °C for 2 h: ε_r=9.9, $Q\times f$=124,147 GHz, tanδ=7.98 × 10^{-5}, and τ_f=−56 ppm/°C. The higher densification benefits the $Q\times f$. However, Raman and FT-IR analysis on Sc^{3+} modified $ZnGa_2O_4$ further elucidated that when the relative density is almost the same, the short-range cation ordering degree is the dominant factor to $Q\times f$. The Raman and FT-IR shift further confirmed bond vibration induced by Sc^{3+} modification. The tanδ was found to follow closely with the FWHM of A_{1g} and T_{2g} modes, which represents the short-range cation ordering degree. The highest $Q\times f$ value for 5Cr-ZGO can be attributed to the highest short-range cation ordering degree and the highest density, while the decrease of $Q\times f$ of 7Sc-ZGO can be ascribed to the decrease of short-range cation ordering degree and lower density. Thus, tiny Sc^{3+} (ppt) modification can greatly improve both $Q\times f$ and τ_f of $ZnGa_2O_4$ ceramics.

CRediT authorship contribution statement

Xiaochi Lu: Conceptualization, Methodology, Software, Validation, Data curation, Writing - original draft. **Bin Quan:** Investigation. **Kailai Zheng:** Resources. **Peng Chu:** Visualization. **Jian Wang:** Formal analysis. **Guangxu Shen:** Writing - review & editing. **Qitu Zhang:** Supervision. **Feng Xu:** Supervision.

Declaration of Competing Interest

The authors declare that they have no known competing financial interests or personal relationships that could have appeared to influence the work reported in this paper.

Acknowledgement

This work was supported in part by the open research fund of the National and Local Joint Engineering Laboratory of RF Integration and Micro-Assembly Technology (Grant Nos. KFJJ20180205, KFJJ20200204), the NUPTSF (Grant No. NY220125, NY218113, NY219077), the Opening Project of the State Key Laboratory of High-Performance Ceramics and Superfine Microstructure (Project no. SKL201 309SIC), and the Open Research Program Of State Key Lab. Of Millimeter Waves In Southeast University (K201928).

References

[1] H. Ji, X. Hou, M.S. Molokeev, J. Ueda, S. Tanabe, M.G. Brik, Ultrabroadband red luminescence of Mn^{4+} in $MgAl_2O_4$ peaking at 651 nm, Dalton Trans. 49 (2020) 5711–5721.
[2] T.A. Safeera, J. Johny, S. Shaji, Y.T. Nien, E.I. Anila, Impact of activator incorporation on red emitting rods of $ZnGa_2O_4$:Cr^{3+} phosphor, Mater. Sci. Eng. 94 (2019) 1037–1043.
[3] A. Saad, H. Shen, Z. Cheng, Q. Ju, M. Yang, Three-dimensional mesoporous phosphide-spinel oxide heterojunctions with dual function as catalysts for overall water splitting, ACS Appl. Energy Mater. 3 (2020) 1684–1693.
[4] F. Gao, C. Chu, W. Zhu, X. Tang, H. Yi, High-efficiency catalytic oxidation of nitric oxide over spherical Mn Co spinel catalyst at low temperature, Appl. Surf. Sci. 479 (2019) 548–556.
[5] D.H. Kim, S. Ning, C.A. Ross, Self-assembled multiferroic perovskite–spinel nanocomposite thin films: epitaxial growth, templating and integration on silicon, J. Mater. Chem. C 7 (2019) 9128–9148.
[6] A. Sahu, R. Chaurashiya, K. Hiremath, A. Dixit, Nanostructured zinc titanate wide band gap semiconductor as a photoelectrode material for quantum dot sensitized solar cells, Sol. Energy 163 (2018) 338–346.
[7] Z. Wei, G. He, W. Hu, Z. Feng, K. Jin, Anomalies of upper critical field in the spinel superconductorLiTi2O4−δ, Phys. Rev. B 100 (2019) 184509.
[8] K. Jin, G. He, X. Zhang, S. Maruyama, S. Yasui, R. Suchoski, Anomalous magnetoresistance in the spinel superconductor $LiTi_2O_4$, Nat. Commun. 6 (2015) 7183.
[9] W.J. Bian, X.C. Lu, Y. Wang, H.K. Zhu, T. Chen, S.W. Ta, Q.T. Zhang, Correlations between structure and microwave dielectric properties of Co doped $MgMoO_4$ ceramics, Ceram. Int. 46 (2020) 22024–22029.
[10] W.J. Bian, X.C. Lu, Y.Y. Li, C.F. Min, H.K. Zhu, Z.X. Fu, Q.T. Zhang, Influence of Nd doping on microwave dielectric properties of $SrTiO_3$ ceramics, J. Mater. Sci. Mater. Electron. 29 (2018) 2743–2747.
[11] A. Kan, T. Moriyama, S. Takahashi, H. Ogawa, Cation distributions and microwave dielectric properties of spinel-structured $MgGa_2O_4$ ceramics, Jpn. J. Appl. Phys. 52 (2013) 09KH01.
[12] S. Takahashi, A. Kan, H. Ogawa, Microwave dielectric properties and crystal structures of spinel structured $MgAl_2O_4$ ceramics synthesized by a molten-salt method, J. Eur. Ceram. Society 37 (2016) 1001–1006.
[13] Y.C. Chen, H.M. You, K.C. Chang, Influence of Li_2WO_4, aid and sintering temperature on microstructures and microwave dielectric properties of Zn_2SnO_4 ceramics, Ceram. Int. 41 (2014) 5257–5262.
[14] R.Z. Zuo, J. Zhang, J. Song, Y.D. Xu, Liquid-phase sintering, microstructural evolution and microwave dielectric properties of $Li_2Mg_3SnO_6$-LiF ceramics, J. Am. Ceram. Soc. 101 (2017) 569–576.
[15] X.L. Jing, X.L. Tang, W.H. Tang, Y.L. Jing, H. Su, Effects of Zn2+ substitution on the sintering behaviour and dielectric properties of Li2Mg1−xZnxSiO4 ceramics, Appl. Phys. A 125 (2019) 415.
[16] H.W. Chen, H. Su, H.W. Zhang, T.C. Zhou, B.W. Zhang, J.F. Zhang, X.L. Tang, Low-temperature sintering and microwave dielectric properties of $(Zn_{1-x}Co_x)_2SiO_4$ ceramics, Ceram. Int. 40 (2014) 14655–14659.
[17] X.K. Lan, J. Li, Z.T. Zou, M.K. Xie, W. Lei, Improved sinterability and microwave dielectric properties of $[Zn_{0.5}Ti_{0.5}]^{3+}$ doped $ZnAl_2O_4$ spinel solid solution, J. Am. Ceram. Soc. 102 (2019) 5952–5957.
[18] S. Takahashi, A. Kan, H. Ogawa, Microwave dielectric properties and crystal structures of $Mg_{0.7}Al_{2.2}O_4$ and $Mg_{0.4}Al_{2.4}O_4$ ceramics with defect structures, J. Am. Ceram. Soc. 100 (2017) 3497–3504.
[19] X.C. Lu, W.J. Bian, B. Quan, Z.F. Wang, H.K. Zhu, Q.T. Zhang, Compositional tailoring effect on $ZnGa_2O_4$-TiO_2 ceramics for tunable microwave dielectric properties, J. Alloy. Compd. 792 (2019) 742–749.
[20] X.C. Lu, W.J. Bian, C.F. Min, Z.X. Fu, Q.T. Zhang, H.K. Zhu, Cation distribution of high-performance Mn-substituted $ZnGa_2O_4$ microwave dielectric ceramics, Ceram. Int. 44 (2018) 10028–10034.
[21] X.C. Lu, Z.H. Du, B. Quan, W.J. Bian, H.K. Zhu, Q.T. Zhang, Structural dependence of microwave dielectric properties of Cr^{3+}-substituted $ZnGa_2O_4$ spinel ceramics: crystal distortion and vibration modes study, J. Mater. Chem. C. 7 (2019) 8261–8268.
[22] X.C. Lu, W.J. Bian, Y.Y. Li, H.K. Zhu, Z.X. Fu, Q.T. Zhang, Influence of inverse spinel structured $CuGa_2O_4$ on microwave dielectric properties of normal spinel $ZnGa_2O_4$ ceramics, J. Am. Ceram. Soc. 101 (2018) 1646–1654.
[23] X.C. Lu, W.J. Bian, Y.Y. Li, H.K. Zhu, Z.X. Fu, Q.T. Zhang, Cation distributions and microwave dielectric properties of Cu-substituted $ZnGa_2O_4$ spinel ceramics, Ceram. Int. 43 (2017) 13839–13844.
[24] S. Zhang, H. Sahin, E. Torun, F. Peeters, D. Martien, T. Dapron, N. Dilley, N. Newman, Fundamental mechanisms responsible for the temperature coefficient of resonant frequency in microwave dielectric ceramics, J. Am. Ceram. Soc. 100 (2017) 1508–1516.
[25] M.T. Sebastian, Dielectric materials for wireless communication, J. Mater. Chem. 11 (2010) 54–62.
[26] N. Udomkan, P. Limsuwan, T. Tunkasiri, Effect of rare-earth (RE = La, Nd, Ce and Gd) doping on the piezoelectric of PZT(52:48) ceramics, Int. J. Mod. Phys. B 21 (2009) 4549–4559.
[27] J. Takahashi, T. Ikegami, K. Kageyama, Occurrence of dielectric 1:1:4 compound in the ternary system BaO-Ln_2O_3-TiO_2 (Ln = La, Nd, and Sm): II, reexamination of formation of isostructural ternary compounds in identical systems, J. Am. Ceram. Soc. 74 (1991) 1868–1872.

[28] Hisakazu Takahashi, Yoko Baba, Kenichi Ezaki, Microwave dielectric properties and crystal structure of CaO-Li_2O-(1-x)Sm_2O_3-xLn_2O_3-TiO_2 (Ln: lanthanide) ceramics system, Jpn. J. Appl. Phys. 9B (1996) 5069–5073.
[29] X.C. Fan, X.M. Chen, X.Q. Liu, Complex-permittivity measurement on high-Q materials via combined numerical approaches, IEEE Trans. Microw. Theory Tech. 53 (2005) 3130–3134.
[30] S.P. Wu, J.J. Xue, R. Wang, J.H. Li, Synthesis, characterization and microwave dielectric properties of spinel $MgGa_2O_4$ ceramic materials, J. Alloy. Compd. 585 (2014) 542–548.
[31] R.J. Wiglusz, A. Watras, M. Malecka, P.J. Deren, R. Pazik, Structure evolution and up-conversion studies of ZnX_2O_4:Er^{3+}/Yb^{3+}(X = Al^{3+}, Ga^{3+}, In^{3+}) nanoparticles, Eur. J. Inorg. Chem. 6 (2014) 1090–1101.
[32] M.S. Fu, X.Q. Liu, X.M. Chen, Erratum: giant dielectric response in two-dimensional charge-ordered nickelate ceramics, J. Appl. Phys. 105 (2008) 129902.
[33] C.L. Diao, F. Shi, Correlation among dielectric properties, vibrational modes, and crystal structures in $Ba[Sn_xZn_{(1-x)/3}Nb_{2(1-x)/3}]O_3$ solid solutions, J. Phys. Chem. C 116 (2012) 6852–6858.
[34] F. Shi, H. Dong, Correlation of phonon characteristics and crystal structures of $Ba[Zn_{1/3}(Nb_{1-x}Ta_x)_{2/3}]O_3$ solid solutions, J. Appl. Phys. 111 (2012) 1–5.
[35] F. Shi, H. Dong, Correlation between vibrational modes and structural characteristics of $Ba[(Zn_{1-x}Mg_x)_{1/3}Ta_{2/3}]O_3$ solid solutions, CrystEngComm 14 (2012) 3373–3379.